

Orientational relaxation in a colloidal Heisenberg model

B. U. Felderhof

Institut für Theoretische Physik A, Rheinisch-Westfälische Technische Hochschule Aachen, Templergraben 55, 52056 Aachen, Germany

R. B. Jones

Queen Mary and Westfield College, Department of Physics, Mile End Road, London E1 4NS, Great Britain

(Received 10 February 1993)

We study orientational relaxation in a suspension of directed spheres interacting with a Heisenberg pair interaction. Translational diffusion is neglected. Rotational diffusion is described by a generalized Smoluchowski equation. The wave-number- and frequency-dependent diffusion coefficient characterizing the decay of the rotational dynamic scattering function is calculated to first order in volume fraction. The single-particle orientational correlation function is evaluated to the same order.

PACS number(s): 82.70.Dd, 05.20.Dd, 61.20.Lc, 75.10.Nr

I. INTRODUCTION

Orientational relaxation of molecules in liquids can be observed by various experimental methods [1]. Due to the complexity of the coupling of translational and rotational motions, the theory is less well developed than the theory of atomic liquids [2]. Most effort has been directed towards the study of dielectric relaxation [2–8].

In the following we investigate a simple model in which translational motion is completely neglected. We consider a suspension of oriented spheres which interact via a distance-dependent Heisenberg pair interaction. The diffusion in orientation space is described by a generalized Smoluchowski equation [9]. We neglect hydrodynamic interactions [10,11]. The time correlation function of polarization fluctuations is evaluated as an average over an equilibrium ensemble of positions, corresponding to a disordered system.

In a previous article [12] we have derived general expressions for the time correlation function of polarization fluctuations and the single-particle orientational relaxation function of a colloidal suspension of spheres, valid to first order in volume fraction. Here we show that for the Heisenberg model these expressions can be evaluated exactly. The explicit results contain a wealth of information on the process of orientational relaxation. For Heisenberg interaction of moderate strength, at least four relaxation times are necessary for an accurate description of the memory function characterizing the frequency dependence of the rotational diffusion coefficient. The rotational dynamic scattering function for ferromagnetic Heisenberg interaction is markedly different from that for antiferromagnetic interaction.

The present model is of interest as the classical limit of spin-glass systems studied in solid-state physics [13]. However, the Heisenberg interaction is not very realistic for actual colloidal suspensions. Nonetheless, the model serves as a useful guide in the study of real physical systems. We have employed the method developed here in the study of liquid crystals and ferrofluids. We hope to report on that work in future presentations.

II. DESCRIPTION OF THE MODEL

We consider N spherical particles immersed in a fluid at temperature T . The whole system is enclosed in a volume Ω . The orientation of a sphere is indicated by the direction of a unit vector \mathbf{u} at its center. The spheres are assumed to interact via a direct pair potential of the form

$$v(r, \mathbf{u}_1, \mathbf{u}_2) = v_0(r) + J(r) \mathbf{u}_1 \cdot \mathbf{u}_2, \quad (1)$$

where $r = |\mathbf{R}_2 - \mathbf{R}_1|$ is the distance between the centers of two spheres. Hydrodynamic interactions will be neglected. If \mathbf{R}_i denotes the position of the i th sphere, and \mathbf{u}_i its orientation, then the positions of all spheres are described by the $3N$ -dimensional vector $\mathbf{X}_T = (\mathbf{R}_1, \dots, \mathbf{R}_N)$, and the orientations are described by the $3N$ -dimensional vector $\mathbf{X}_R = (\mathbf{u}_1, \dots, \mathbf{u}_N)$. The total configuration is summarized in the $6N$ -dimensional vector $\mathbf{X} = (\mathbf{X}_T, \mathbf{X}_R)$. In Eq. (1) negative J implies ferromagnetic interaction. In solid-state physics, the Heisenberg interaction between two spins is usually defined with the opposite sign.

We consider an ensemble of configurations \mathbf{X} , described by a time-dependent probability distribution $P(\mathbf{X}, t)$, which obeys the generalized Smoluchowski equation [9–11]. We assume that rotational diffusion is fast compared with translational diffusion. On the basis of the separation of time scales, we study the relaxation of orientations for a fixed set of positions \mathbf{X}_T . Finally, we average over an equilibrium ensemble of positions \mathbf{X}_T . Thus we approximate the distribution function by

$$P(\mathbf{X}, t) = P_{\text{Teq}}(\mathbf{X}_T) P_R(\mathbf{X}_R, t; \mathbf{X}_T), \quad (2)$$

where $P_{\text{Teq}}(\mathbf{X}_T)$ is the equilibrium distribution of positions and $P_R(\mathbf{X}_R, t; \mathbf{X}_T)$ is the orientational distribution function for fixed positions \mathbf{X}_T . We assume that the latter obeys the generalized Smoluchowski equation

$$\frac{\partial P_R}{\partial t} = \mathcal{D} P_R, \quad (3)$$

where \mathcal{D} is the Smoluchowski operator defined by

$$\mathcal{D}P_R = D_R \underline{L} \cdot [\underline{L}P_R + \beta(\underline{L}\Phi)P_R] . \quad (4)$$

Here, D_R is the rotational diffusion coefficient for a single sphere, and $\underline{L} = (\underline{L}_1, \dots, \underline{L}_N)$ is a rotation operator with components for sphere j :

$$\underline{L}_j = \mathbf{u}_j \times \frac{\partial}{\partial \mathbf{u}_j} . \quad (5)$$

Furthermore, $\beta = 1/k_B T$ and the potential $\Phi(\mathbf{X})$ incorporates both a wall potential and the direct pair interaction (1). The Smoluchowski equation (3) describes how the distribution function $P_R(\mathbf{X}_R, t; \mathbf{X}_T)$ tends to the equilibrium distribution

$$P_{R\text{eq}}(\mathbf{X}_R; \mathbf{X}_T) = \exp[-\beta\Phi(\mathbf{X})]/Z_R(\beta; \mathbf{X}_T) \quad (6)$$

in the course of time. The partition function $Z_R(\beta; \mathbf{X}_T)$ normalizes the distribution to unity. The complete equilibrium distribution is given by

$$P_{\text{eq}}(\mathbf{X}) = P_{T\text{eq}}(\mathbf{X}_T) P_{R\text{eq}}(\mathbf{X}_R; \mathbf{X}_T) . \quad (7)$$

We consider equilibrium fluctuations of polarization at wave vector \mathbf{k} . The corresponding variable is

$$\mathbf{M}(\mathbf{k}) = \mu \sum_{j=1}^N \mathbf{u}_j e^{-i\mathbf{k} \cdot \mathbf{R}_j} , \quad (8)$$

where μ is the dipole strength. The time-dependent orientational scattering function is defined by

$$\mathbf{F}_R(\mathbf{k}, t) = \lim_{\substack{N \rightarrow \infty \\ \Omega \rightarrow \infty}} \frac{1}{N} \langle \mathbf{M}(\mathbf{k}, t) \mathbf{M}(-\mathbf{k}) \rangle , \quad (9)$$

where the time dependence is governed by the adjoint Smoluchowski operator \mathcal{L} , such that

$$\mathbf{M}(\mathbf{k}, t) = \exp(\mathcal{L}t) \mathbf{M}(\mathbf{k}, 0) , \quad \mathbf{M}(\mathbf{k}, 0) = \mathbf{M}(\mathbf{k}) . \quad (10)$$

The operator \mathcal{L} is given by

$$\mathcal{L} = D_R [\underline{L} - \beta(\underline{L}\Phi)] \cdot \underline{L} . \quad (11)$$

The angular brackets in Eq. (9) indicate an average over the equilibrium distribution (7). Finally, we take the thermodynamic limit $N \rightarrow \infty$, $\Omega \rightarrow \infty$ at constant $n_0 = N/\Omega$. Since there are no applied fields, the system is homogeneous and isotropic in the thermodynamic limit.

The one-sided Fourier transform of the scattering function is given by

$$\mathbf{G}_R(\mathbf{k}, \omega) = n_0 \int_0^\infty e^{i\omega t} \mathbf{F}_R(\mathbf{k}, t) dt . \quad (12)$$

From Eqs. (9) and (10) we find the expression

$$G_{R\alpha\beta}(\mathbf{k}, \omega) = \lim_{\substack{N \rightarrow \infty \\ \Omega \rightarrow \infty}} \frac{-1}{\Omega} \langle M_\beta(-\mathbf{k}) [i\omega + \mathcal{L}]^{-1} M_\alpha(\mathbf{k}) \rangle . \quad (13)$$

The (\mathbf{k}, ω) -dependent diffusion tensor $\mathbf{D}_R(\mathbf{k}, \omega)$ is defined by

$$\mathbf{G}_R(\mathbf{k}, \omega) = k_B T [-i\omega \mathbf{1} + 2\mathbf{D}_R(\mathbf{k}, \omega)]^{-1} \cdot \chi^0(\mathbf{k}, 0) , \quad (14)$$

where $\chi^0(\mathbf{k}, 0)$ is the zero-frequency susceptibility tensor

$$\chi^0(\mathbf{k}, 0) = \lim_{\substack{N \rightarrow \infty \\ \Omega \rightarrow \infty}} \frac{\beta}{\Omega} \langle \mathbf{M}(\mathbf{k}) \mathbf{M}(-\mathbf{k}) \rangle . \quad (15)$$

By isotropy, the diffusion tensor takes the form

$$\mathbf{D}_R(\mathbf{k}, \omega) = D_{Rl}(k, \omega) \hat{\mathbf{k}} \hat{\mathbf{k}} + D_{Rt}(k, \omega) (1 - \hat{\mathbf{k}} \hat{\mathbf{k}}) . \quad (16)$$

The susceptibility tensor takes the form

$$\chi^0(\mathbf{k}, 0) = \frac{1}{3} \beta n_0 \mu^2 [S_l(k) \hat{\mathbf{k}} \hat{\mathbf{k}} + S_t(k) (1 - \hat{\mathbf{k}} \hat{\mathbf{k}})] , \quad (17)$$

with static structure factors $S_l(k)$ and $S_t(k)$. Clearly, the scattering function can also be decomposed into longitudinal and transverse parts.

III. SHORT-TIME ROTATIONAL DIFFUSION

In the following we restrict ourselves to consideration of a semidilute suspension. The diffusion tensor $\mathbf{D}_R(\mathbf{k}, \omega)$ will be evaluated to first order in the volume fraction occupied by spheres. The susceptibility tensor $\chi^0(\mathbf{k}, 0)$ will be evaluated to second order.

We consider first the susceptibility tensor. The structure factors $S_l(k)$ and $S_t(k)$ are given by

$$\begin{aligned} S_l(k) &= 1 + \frac{1}{3} n_0 [\hat{h}_\Delta(k) + 2\bar{h}_D(k)] , \\ S_t(k) &= 1 + \frac{1}{3} n_0 [\hat{h}_\Delta(k) - \bar{h}_D(k)] , \end{aligned} \quad (18)$$

where $\hat{h}_D(k)$ is the Fourier transform of the pair-correlation function $h_\Delta(r)$, and $\bar{h}_D(k)$ is the Hankel transform of the pair-correlation function $h_D(r)$, as defined in Hansen and McDonald [2]. To zeroth order in volume fraction, the pair-correlation functions are given by

$$\begin{aligned} h_\Delta(r) &= \frac{3}{16\pi^2} \int \mathbf{u}_1 \cdot \mathbf{u}_2 [e^{-\beta v} - 1] d\mathbf{u}_1 d\mathbf{u}_2 , \\ h_D(r) &= \frac{3}{32\pi^2} \int [3\mathbf{u}_1 \cdot \hat{\mathbf{r}} \hat{\mathbf{r}} \cdot \mathbf{u}_2 - \mathbf{u}_1 \cdot \mathbf{u}_2] [e^{-\beta v} - 1] d\mathbf{u}_1 d\mathbf{u}_2 . \end{aligned} \quad (19)$$

For our system the function $h_D(r)$ vanishes due to isotropy. The transform $\hat{h}_\Delta(k)$ in Eq. (18) is given by

$$\hat{h}_\Delta(k) = 4\pi \int_0^\infty j_0(kr) h_\Delta(r) r^2 dr . \quad (20)$$

In order to evaluate the integral, we consider the two-particle distribution

$$f(\mathbf{u}_1, \mathbf{u}_2) = \frac{1}{16\pi^2} \exp[-K \mathbf{u}_1 \cdot \mathbf{u}_2] / Y_0(K) , \quad (21)$$

with normalization integral

$$Y_0(K) = \frac{1}{16\pi^2} \int \exp[-K \mathbf{u}_1 \cdot \mathbf{u}_2] d\mathbf{u}_1 d\mathbf{u}_2 . \quad (22)$$

The latter is easily evaluated as

$$Y_0(K) = \frac{\sinh K}{K} . \quad (23)$$

One also finds

$$\langle \mathbf{u}_1 \rangle_K = \langle \mathbf{u}_2 \rangle_K = 0 , \quad (24)$$

where the angular brackets with subscript K indicate an average over the distribution $f(\mathbf{u}_1, \mathbf{u}_2)$. Furthermore,

$$\langle \mathbf{u}_1 \mathbf{u}_2 \rangle_K = \frac{1}{3} \left[\frac{1}{K} - \coth K \right] \mathbf{1}. \quad (25)$$

Using these results in Eq. (19), one finds

$$h_\Delta(r) = 3 \exp[-\beta v_0(r)] Y_1[\beta J(r)], \quad (26)$$

where

$$Y_1(K) = -\frac{dY_0}{dK} = \frac{\sinh K}{K^2} - \frac{\cosh K}{K}. \quad (27)$$

The function $Y_1(K)$ is odd in K and vanishes at $K=0$.

For hard spheres of hard-core radius a , the volume fraction is defined as $\phi = (4\pi/3)n_0 a^3$. To first order in volume fraction, the diffusion tensor is written as

$$\mathbf{D}_R(\mathbf{k}, \omega) = D_R \{ \mathbf{1} + [\lambda_R(\mathbf{k}) + \alpha_R(\mathbf{k}, \omega)] \phi \}, \quad (28)$$

with a tensor $\alpha_R(\mathbf{k}, \omega)$ which tends to zero at high frequency, so that $\lambda_R(\mathbf{k})$ represents the density correction at high frequency. The tensor $\lambda_R(\mathbf{k})$ may be expressed in terms of the static structure factors. We have shown elsewhere [12] that at any density the high-frequency limit of the diffusion tensor is given by

$$\mathbf{D}_R^S(\mathbf{k}) = \frac{D_R}{S_l(k)} \hat{\mathbf{k}} \hat{\mathbf{k}} + \frac{D_R}{S_l(k)} (1 - \hat{\mathbf{k}} \hat{\mathbf{k}}). \quad (29)$$

Substituting from Eq. (18) and using the vanishing of $h_D(r)$, we find that the tensor $\lambda_R(\mathbf{k})$ is given by

$$\lambda_R(\mathbf{k}) = \lambda_R(k) \mathbf{1}, \quad \lambda_R(k) = -\frac{1}{4\pi a^3} \hat{h}_\Delta(k). \quad (30)$$

This represents a virial-type correction to the diffusion coefficient. For purely ferromagnetic interaction [$J(r) < 0$], the scalar $\lambda_R(0)$ is negative; for purely antiferromagnetic interaction, it is positive. To give a numerical example, we consider an interaction $v_0(r)$, which vanishes for $r > 2a$ and is infinite for $r < 2a$, and an interaction $J(r)$ which takes the constant value J in the range $2a < r < 2x_1 a$ and vanishes elsewhere. For this interaction we find

$$\lambda_R(0) = -8(x_1^3 - 1) Y_1(\beta J). \quad (31)$$

This shows that for $\beta J \approx -1$ and $x_1 \approx 2$, the interactions cause an appreciable slowing down of collective rotational diffusion. For antiferromagnetic interaction of the same magnitude, the rotational diffusion is speeded up. We recall that the short-time rotational diffusion of a single sphere is not affected by the interactions [12].

IV. MEMORY EFFECTS

The dependence of the rotational diffusion tensor on frequency is due to memory effects. In this section we discuss the frequency dependence to first order in volume fraction, as given by the tensor $\alpha_R(\mathbf{k}, \omega)$, defined in Eq. (28). The tensor may be calculated from a solution of the two-sphere Smoluchowski equation. We shall show that, like the tensor $\lambda_R(\mathbf{k})$, it is proportional to the unit tensor.

We introduce the scalar product between two functions $A(\mathbf{r}, \mathbf{u}_1, \mathbf{u}_2)$ and $B(\mathbf{r}, \mathbf{u}_1, \mathbf{u}_2)$ as

$$(A|B) = \frac{1}{16\pi^2} \int g(\mathbf{r}, \mathbf{u}_1, \mathbf{u}_2) A^*(\mathbf{r}, \mathbf{u}_1, \mathbf{u}_2) B(\mathbf{r}, \mathbf{u}_1, \mathbf{u}_2) \times d\mathbf{r} d\mathbf{u}_1 d\mathbf{u}_2, \quad (32)$$

with weight factor

$$g(\mathbf{r}, \mathbf{u}_1, \mathbf{u}_2) = \exp[-\beta v(\mathbf{r}, \mathbf{u}_1, \mathbf{u}_2)]. \quad (33)$$

We define the two-body Smoluchowski operator for two spheres centered at $\mathbf{R}_1, \mathbf{R}_2$ with distance vector $\mathbf{r} = \mathbf{R}_2 - \mathbf{R}_1$ as

$$\mathcal{L}_r = D_R [\underline{L} - \beta(\underline{L}v)] \cdot \underline{L}, \quad (34)$$

with $\underline{L} = (\mathbf{L}_1, \mathbf{L}_2)$. The corresponding operator $D_R \underline{L}^2$ for free diffusion is denoted as \mathcal{L}_{fr} . The perturbation operator V_r is defined as the difference

$$V_r = \mathcal{L}_r - \mathcal{L}_{fr} = -\beta D_R (\underline{L}v) \cdot \underline{L}. \quad (35)$$

We abbreviate

$$|\mathbf{k}\rangle = \mathbf{u}_1 e^{i\mathbf{k}\cdot\mathbf{r}/2} + \mathbf{u}_2 e^{-i\mathbf{k}\cdot\mathbf{r}/2}. \quad (36)$$

We have shown elsewhere [12] that with this notation the tensor $\lambda_R(\mathbf{k})$ may be expressed as

$$\lambda_R(\mathbf{k}) = -\frac{9}{16\pi a^3 D_R} (\mathbf{k}|V_r|\mathbf{k}). \quad (37)$$

We abbreviate

$$|V\mathbf{k}\rangle = V_r |\mathbf{k}\rangle = U_r(\mathbf{k}). \quad (38)$$

We have also shown [12] that the tensor $\alpha_R(\mathbf{k}, \omega)$ may be expressed as

$$\alpha_R(\mathbf{k}, \omega) = \frac{9}{16\pi a^3 D_R} \left[V\mathbf{k} \left| \frac{1}{i\omega + \mathcal{L}_r} \right| V\mathbf{k} \right]. \quad (39)$$

In order to evaluate the effect of the inverse operator, we must solve the two-sphere Smoluchowski equation. This is conveniently done in a matrix representation of the operator.

It turns out that for the chosen interaction (1) the matrix representation is relatively simple. For this interaction the perturbation operator V_r is given by

$$V_r = -D_R K(r) (\mathbf{u}_1 \times \mathbf{u}_2) \cdot (\mathbf{L}_1 - \mathbf{L}_2), \quad (40)$$

with $K(r) = \beta J(r)$. We define the vector functions

$$\begin{aligned} \mathbf{P}_l^{(1)}(\mathbf{u}_1, \mathbf{u}_2) &= (\mathbf{u}_1 \cdot \mathbf{u}_2)^{l-1} \mathbf{u}_1, \\ \mathbf{P}_l^{(2)}(\mathbf{u}_1, \mathbf{u}_2) &= (\mathbf{u}_1 \cdot \mathbf{u}_2)^{l-1} \mathbf{u}_2, \end{aligned} \quad (41)$$

for integer $l = 1, 2, \dots$. The action of the free diffusion operator on the first function is given by

$$\begin{aligned} (L_1^2 + L_2^2) \mathbf{P}_l^{(1)} &= 2(l-1)(l-2) \mathbf{P}_l^{(1)} \\ &\quad + 2(l-1) \mathbf{P}_{l-1}^{(2)} - 2l^2 \mathbf{P}_l^{(1)}. \end{aligned} \quad (42)$$

The action of the operator appearing in Eq. (40) is given by

$$\begin{aligned} (\mathbf{u}_1 \times \mathbf{u}_2) \cdot (\mathbf{L}_1 - \mathbf{L}_2) \mathbf{P}_l^{(1)} \\ = 2(l-1) \mathbf{P}_{l-1}^{(1)} + \mathbf{P}_l^{(2)} - (2l-1) \mathbf{P}_{l+1}^{(1)}. \end{aligned} \quad (43)$$

The action of the operators on the function $\mathbf{P}_l^{(2)}$ is found by an interchange of superscripts (1) and (2) in Eqs. (42) and (43). It is evident that we can evaluate the expression in Eq. (39) in a matrix representation defined by the functions (41).

V. MATRIX REPRESENTATION

In order to find the matrix representation of the expression in Eq. (39), we consider the equation

$$[i\omega + \mathcal{L}_r] \psi_r(\mathbf{k}) = \mathbf{U}_r(\mathbf{k}). \quad (44)$$

By linearity we can put

$$\psi_r(\mathbf{k}) = \psi^{(1)} e^{i\mathbf{k}\cdot\mathbf{r}/2} + \psi^{(2)} e^{-i\mathbf{k}\cdot\mathbf{r}/2}, \quad (45)$$

where $\psi^{(1)}$ satisfies the equation

$$[i\omega + \mathcal{L}_r] \psi^{(1)} = \mathbf{U}^{(1)}, \quad (46)$$

with $\mathbf{U}^{(1)}$ defined by

$$\mathbf{U}^{(1)} = V_r \mathbf{u}_1, \quad \mathbf{U}^{(2)} = V_r \mathbf{u}_2. \quad (47)$$

The solution $\psi^{(2)}$ is obtained by interchange of superscripts (1) and (2). We expand the function $\psi^{(1)}$ as

$$\begin{aligned} \psi^{(1)}(\mathbf{u}_1, \mathbf{u}_2, \omega) = \sum_{l=1}^{\infty} [A_l^{(11)}(\omega) \mathbf{P}_l^{(1)}(\mathbf{u}_1, \mathbf{u}_2) \\ + A_l^{(12)}(\omega) \mathbf{P}_l^{(2)}(\mathbf{u}_1, \mathbf{u}_2)] \end{aligned} \quad (48)$$

and the function $\mathbf{U}^{(1)}$ as

$$\begin{aligned} \mathbf{U}^{(1)}(\mathbf{u}_1, \mathbf{u}_2) = D_R \sum_{l=1}^{\infty} [U_l^{(11)} \mathbf{P}_l^{(1)}(\mathbf{u}_1, \mathbf{u}_2) \\ + U_l^{(12)} \mathbf{P}_l^{(2)}(\mathbf{u}_1, \mathbf{u}_2)]. \end{aligned} \quad (49)$$

We define matrices \underline{M} and \underline{N} by

$$\mathcal{L}_r \mathbf{P}_l^{(1)} = -D_R \sum_{l'=1}^{\infty} [M_{ll'} \mathbf{P}_l^{(1)} + N_{ll'} \mathbf{P}_l^{(2)}]. \quad (50)$$

By interchange of superscripts,

$$\mathcal{L}_r \mathbf{P}_l^{(2)} = -D_R \sum_{l'=1}^{\infty} [N_{ll'} \mathbf{P}_l^{(1)} + M_{ll'} \mathbf{P}_l^{(2)}]. \quad (51)$$

In matrix representation Eq. (46) becomes

$$i\omega A_l^{(11)} - D_R \sum_{l'=1}^{\infty} [M_{ll'} A_{l'}^{(11)} + N_{ll'} A_{l'}^{(12)}] = D_R U_l^{(11)}, \quad (52)$$

$$i\omega A_l^{(12)} - D_R \sum_{l'=1}^{\infty} [N_{ll'} A_{l'}^{(11)} + M_{ll'} A_{l'}^{(12)}] = D_R U_l^{(12)}.$$

Adding and subtracting the equations, we get

$$i\omega A_l^{1\pm} - D_R \sum_{l'=1}^{\infty} M_{ll'}^{\pm} A_{l'}^{1\pm} = D_R U_l^{1\pm}, \quad (53)$$

with the definitions

$$A_l^{1\pm} = A_l^{(11)} \pm A_l^{(12)}, \quad U_l^{1\pm} = U_l^{(11)} \pm U_l^{(12)}, \quad (54)$$

$$\underline{M}^{\pm} = \underline{M} \pm \underline{N}.$$

By interchange of superscripts, we get

$$\begin{aligned} \psi^{(2)}(\mathbf{u}_1, \mathbf{u}_2, \omega) = \sum_{l=1}^{\infty} [A_l^{(21)}(\omega) \mathbf{P}_l^{(1)}(\mathbf{u}_1, \mathbf{u}_2) \\ + A_l^{(22)}(\omega) \mathbf{P}_l^{(2)}(\mathbf{u}_1, \mathbf{u}_2)], \end{aligned} \quad (55)$$

with coefficients given by

$$A_l^{(21)}(\omega) = A_l^{(12)}(\omega), \quad A_l^{(22)}(\omega) = A_l^{(11)}(\omega). \quad (56)$$

Hence it follows that the upper sign in Eq. (54) corresponds to the subspace of functions which are even under interchange of particle labels, and the lower sign corresponds to functions which are odd under interchange. From Eqs. (40), (43), and (47), one finds

$$\mathbf{U}^{(1)} = -D_R K [\mathbf{u}_2 - (\mathbf{u}_1 \cdot \mathbf{u}_2) \mathbf{u}_1], \quad (57)$$

so that

$$U_l^{(11)} = K \delta_{l2}, \quad U_l^{(12)} = -K \delta_{l1}. \quad (58)$$

It suffices to solve the two sets of equations (53). The matrices \underline{M}^{\pm} read explicitly

$$\begin{aligned} M_{ll'}^{\pm} = (2l^2 \pm K) \delta_{ll'} - 2l(l+1) \delta_{l,l'-2} \\ \mp 2l(1 \mp K) \delta_{l,l'-1} - (2l-3)K \delta_{l,l'+1}. \end{aligned} \quad (59)$$

Introducing the variable $s = -i\omega/D_R$, we can write the equations as

$$s A_l^{1\pm} + \sum_{l'=1}^{\infty} M_{ll'}^{\pm} A_{l'}^{\pm} = K [\pm \delta_{l1} - \delta_{l2}]. \quad (60)$$

Substituting the solution $\psi_r(\mathbf{k})$, given by Eqs. (45), (48), and (55), back into Eq. (39), we perform the angular averages to get

$$\begin{aligned} \langle \mathbf{u}_1 \mathbf{P}_l^{(1)} \rangle_K = \langle \mathbf{u}_2 \mathbf{P}_l^{(2)} \rangle_K = \frac{Y_{l-1}(K)}{3Y_0(K)} \mathbf{1}, \\ \langle \mathbf{u}_1 \mathbf{P}_l^{(2)} \rangle_K = \langle \mathbf{u}_2 \mathbf{P}_l^{(1)} \rangle_K = \frac{Y_l(K)}{3Y_0(K)} \mathbf{1}, \end{aligned} \quad (61)$$

where the function $Y_l(K)$ is defined as the integral

$$Y_l(K) = \frac{1}{16\pi^2} \int (\mathbf{u}_1 \cdot \mathbf{u}_2)^l \exp(-K \mathbf{u}_1 \cdot \mathbf{u}_2) d\mathbf{u}_1 d\mathbf{u}_2. \quad (62)$$

This generalizes the definitions (22) and (25). Clearly,

$$Y_l(K) = \left[-\frac{d}{dK} \right]^l \frac{\sinh K}{K}. \quad (63)$$

The functions $Y_l(K)$ are given by

$$\begin{aligned} Y_l(K) = \left[\sum_{m=1}^{l+1} f(l, m) K^{-m} \right] \sinh K \\ - \left[\sum_{m=1}^l g(l, m) K^{-m} \right] \cosh K, \end{aligned} \quad (64)$$

with coefficients which follow from the recursion relations

$$\begin{aligned} f(l, m) = (m-1)f(l-1, m-1) + g(l-1, m), \\ g(l, m) = (m-1)g(l-1, m-1) + f(l-1, m), \end{aligned} \quad (65)$$

with initial values

$$f(1,1)=0, \quad f(1,2)=1, \quad g(1,1)=1. \quad (66)$$

The angular integration in Eq. (39) yields

$$\begin{aligned} & \frac{1}{16\pi^2} \int \exp[-K\mathbf{u}_1 \cdot \mathbf{u}_2] \mathbf{U}_r^*(\mathbf{k}) \psi_r(\mathbf{k}) d\mathbf{u}_1 d\mathbf{u}_2 \\ &= \frac{2}{3} D_R K \mathbf{1} \sum_{l=1}^{\infty} [Y_{l+1}(K) - Y_{l-1}(K)] \\ & \quad \times [A_l^{(11)} \cos \mathbf{k} \cdot \mathbf{r} + A_l^{(12)}]. \end{aligned} \quad (67)$$

This shows that the tensor $\alpha_R(\mathbf{k}, \omega)$ is isotropic:

$$\alpha_R(\mathbf{k}, \omega) = \alpha_R(k, \omega) \mathbf{1}. \quad (68)$$

The scalar $\alpha_R(k, \omega)$ is given by

$$\begin{aligned} \alpha_R(k, \omega) = & \frac{-3}{8\pi a^3} \sum_{l=1}^{\infty} \int e^{-\beta v_0} W_l(K) [A_l^{(11)} \cos \mathbf{k} \cdot \mathbf{r} \\ & + A_l^{(12)}] d\mathbf{r}, \end{aligned} \quad (69)$$

where $W_l(K)$ is defined by

$$W_l(K) = -K [Y_{l+1}(K) - Y_{l-1}(K)]. \quad (70)$$

The integration over angles can be performed and we are finally left with the sum of radial integrals:

$$\begin{aligned} \alpha_R(k, \omega) = & \frac{-3}{2a^3} \sum_{l=1}^{\infty} \int_0^{\infty} e^{-\beta v_0} W_l(K) [A_l^{(11)}(\omega) j_0(kr) \\ & + A_l^{(12)}(\omega)] r^2 dr. \end{aligned} \quad (71)$$

We recall that $K = \beta J(r)$ and that the coefficients $A_l^{(11)}$ and $A_l^{(12)}$ depend on r via K . We conclude this section by casting the scalar $\alpha_R(k, \omega)$ into the final form

$$\alpha_R(k, \omega) = \frac{-3}{2a^3} \int_0^{\infty} e^{-\beta v_0} [\hat{A}(K, \omega) + \hat{B}(K, \omega) j_0(kr)] r^2 dr, \quad (72)$$

with $\hat{A}(K, \omega)$ defined by

$$\hat{A}(K, \omega) = \sum_{l=1}^{\infty} W_l(K) A_l^{(12)}(K, \omega) \quad (73)$$

and $\hat{B}(K, \omega)$ by

$$\hat{B}(K, \omega) = \sum_{l=1}^{\infty} W_l(K) A_l^{(11)}(K, \omega). \quad (74)$$

The coefficients $A_l^{(11)}(K, \omega)$ and $A_l^{(12)}(K, \omega)$ follow from Eqs. (54) and (60).

VI. SYMMETRY

The coefficients $\hat{A}(K, \omega)$ and $\hat{B}(K, \omega)$, introduced in Eqs. (73) and (74), possess an interesting symmetry property with respect to the sign of the Heisenberg interaction. It follows from Eq. (59) that the elements of the matrices \underline{M}^+ and \underline{M}^- are related by

$$M_{ll'}^-(-K) = (-1)^{l+l'} M_{ll'}^+(K). \quad (75)$$

It is easily seen that the solution vectors of Eq. (60) have the related symmetry

$$A_l^{1-}(-K, s) = (-1)^{l+1} A_l^{1+}(K, s). \quad (76)$$

It therefore suffices to consider just one of the sets of equations. We choose the upper sign and simplify notation by dropping superscripts, but add a hat to indicate Laplace transform. The set of equations to be solved reads, therefore,

$$s \hat{A}_l + \sum_{l'=1}^{\infty} M_{ll'} \hat{A}_{l'} = K [\delta_{l1} - \delta_{l2}]. \quad (77)$$

By use of Eq. (54), we find the related symmetry

$$\begin{aligned} A_l^{(11)}(-K, s) &= (-1)^{l+1} A_l^{(11)}(K, s), \\ A_l^{(12)}(-K, s) &= (-1)^l A_l^{(12)}(K, s). \end{aligned} \quad (78)$$

The functions $Y_l(K)$ have the symmetry

$$Y_l(-K) = (-1)^l Y_l(K). \quad (79)$$

From Eqs. (73) and (74) we find the symmetry relations

$$\hat{A}(-K, \omega) = \hat{A}(K, \omega), \quad \hat{B}(-K, \omega) = -\hat{B}(K, \omega). \quad (80)$$

We regard the coefficients $\hat{A}(K, \omega)$ and $\hat{B}(K, \omega)$ as one-sided Fourier transforms of functions $A(K, t)$ and $B(K, t)$,

$$\begin{aligned} \hat{A}(K, \omega) &= \int_0^{\infty} e^{i\omega t} A(K, t) dt, \\ \hat{B}(K, \omega) &= \int_0^{\infty} e^{i\omega t} B(K, t) dt. \end{aligned} \quad (81)$$

From Eq. (80) we find the symmetry property

$$A(-K, t) = A(K, t), \quad B(-K, t) = -B(K, t). \quad (82)$$

It therefore suffices to study the functions $A(K, t)$ and $B(K, t)$ for positive values of K .

In Fig. 1 we plot the coefficients $\hat{A}(K, 0)$ and $\hat{B}(K, 0)$ in

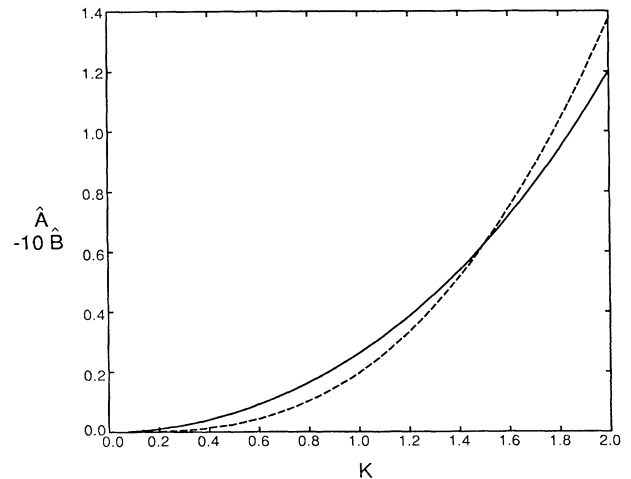


FIG. 1. Plot of the time integrals $\hat{A}(K, 0)$ (solid curve) and $-10\hat{B}(K, 0)$ (dashed curve) as a function of interaction strength K .

the range $0 < K < 2$, as found by numerical solution of Eq. (77) for $s=0$. The values at $K=1$ are

$$\hat{A}(1,0)=0.2617, \quad \hat{B}(1,0)=-0.0197. \quad (83)$$

It suffices to use l values up to $l_{\max}=7$ to achieve the quoted accuracy. At $K=2$,

$$\hat{A}(2,0)=1.2020, \quad \hat{B}(2,0)=-0.1375. \quad (84)$$

One needs l values up to $l_{\max}=10$ to attain the same accuracy.

VII. SINGLE-PARTICLE RELAXATION

Before studying the set of equations (77) in more detail, we note that our calculation also yields information on single-particle relaxation. The orientational correlation function for a single sphere is defined by

$$C^{(1)}(t) = \langle \mathbf{u}_1(t) \cdot \mathbf{u}_1 \rangle, \quad (85)$$

with time evolution governed by the adjoint Smoluchowski operator as in Eq. (10). The integral relaxation time τ_1 is defined by

$$\tau_1 = \int_0^\infty C^{(1)}(t) dt. \quad (86)$$

The one-sided Fourier transform

$$\hat{C}^{(1)}(\omega) = \int_0^\infty e^{i\omega t} C^{(1)}(t) dt \quad (87)$$

may be expressed as

$$\hat{C}^{(1)}(\omega) = \frac{1}{-i\omega + \tau_S^{-1}(\omega)}, \quad (88)$$

with a frequency-dependent relaxation time $\tau_S(\omega)$. We have shown elsewhere [12] that in the absence of hydrodynamic interactions, the relaxation time is given to first order in volume fraction by

$$\tau_S(\omega) = \frac{1}{2D_R} [1 + \alpha_T(\omega)\phi], \quad (89)$$

with a coefficient $\alpha_T(\omega)$ given by

$$\alpha_T(\omega) = \frac{-3}{8\pi a^3 D_R} \left[\mathbf{U}^{(1)} \cdot \left| \frac{1}{i\omega + \mathcal{L}_r} \right| \mathbf{U}^{(1)} \right]. \quad (90)$$

By use of the equations in Sec. V, one finds that this may be expressed as

$$\alpha_T(\omega) = -\alpha_R(\infty, \omega). \quad (91)$$

From Eq. (72) we find for the coefficient $\alpha_R(\infty, \omega)$,

$$\alpha_R(\infty, \omega) = -\frac{3}{2a^3} \int_0^\infty e^{-\beta v_0} \hat{A}(K, \omega) r^2 dr. \quad (92)$$

The integral relaxation time is given by $\tau_1 = \tau_S(0)$. We recall that the short-time relaxation time equals $1/2D_R$.

It follows from the expression (39), and the fact that the Smoluchowski operator \mathcal{L}_r is negative definite, that at zero frequency $\alpha_R(k, 0)$ is negative. In particular, $\alpha_R(\infty, 0)$ is negative, so that the integral relaxation time τ_1 ,

$$\tau_1 = \frac{1}{2D_R} [1 - \alpha_R(\infty, 0)\phi], \quad (93)$$

is always larger than the short-time relaxation time $1/2D_R$. From the symmetry relation (80) it follows that the correction term (92) is even in the sign of the interaction $J(r)$.

We consider again the model studied at the end of Sec. III. For that model,

$$\alpha_R(\infty, 0) = -4(x_1^3 - 1)\hat{A}(\beta J, 0). \quad (94)$$

This shows that the coefficient easily attains appreciable values.

VIII. MEMORY FUNCTION

The time evolution of the scattering function $\mathbf{F}_R(\mathbf{k}, t)$ is expressed conveniently in terms of a memory function. Before studying the scattering function itself, we consider the memory function $\mathbf{M}_R(\mathbf{k}, t)$. It is defined from the integro-differential equation

$$\begin{aligned} \frac{d}{dt} \mathbf{F}_R(\mathbf{k}, t) = & -2\mathbf{D}_R^S(\mathbf{k})\mathbf{F}_R(\mathbf{k}, t) \\ & - \int_0^t \mathbf{M}_R(\mathbf{k}, t-t')\mathbf{F}_R(\mathbf{k}, t') dt'. \end{aligned} \quad (95)$$

Its one-sided Fourier transform

$$\hat{\mathbf{M}}_R(\mathbf{k}, \omega) = \int_0^\infty e^{i\omega t} \mathbf{M}_R(\mathbf{k}, t) dt \quad (96)$$

is found from

$$\mathbf{D}_R(\mathbf{k}, \omega) = \mathbf{D}_R^S(\mathbf{k}) + \frac{1}{2}\hat{\mathbf{M}}_R(\mathbf{k}, \omega). \quad (97)$$

To first order in volume fraction,

$$\hat{\mathbf{M}}_R(\mathbf{k}, \omega) = 2D_R \alpha_R(k, \omega)\phi \mathbf{1}. \quad (98)$$

From Eq. (72) we find

$$\begin{aligned} \mathbf{M}_R(k, t) & \\ & = -3D_R \mathbf{1} \frac{\phi}{a^3} \int_0^\infty e^{-\beta v_0} [A(K, t) + j_0(kr)B(K, t)] r^2 dr. \end{aligned} \quad (99)$$

It clearly suffices to study the functions $A(K, t)$ and $B(K, t)$. From Eq. (60) we find the initial values

$$A(K, 0) = KW_1(K), \quad B(K, 0) = -KW_2(K). \quad (100)$$

Typical values are

$$\begin{aligned} A(1, 0) &= 0.7358, \quad B(1, 0) = 0.1431, \\ A(2, 0) &= 3.8975, \quad B(2, 0) = 1.4074. \end{aligned} \quad (101)$$

$A(K, 0)$ is always larger than $B(K, 0)$. It follows from general properties of the Smoluchowski equation that the function $A(K, t)$, and the expression in square brackets in Eq. (99), decay monotonically with time. In Fig. 2 we plot the initial values $A(K, 0)$ and $B(K, 0)$ in the range $0 < K < 2$. From Eq. (82) it follows that $A(K, 0)$ is even in K , and $B(K, 0)$ is odd in K .

We write $A(K, t)$ and $B(K, t)$ as a sum of two terms,

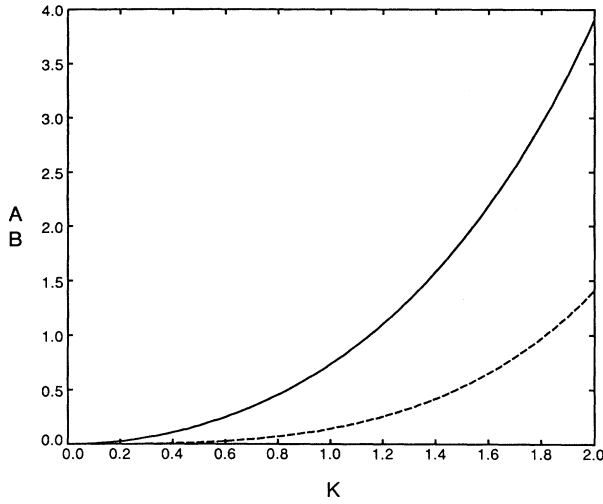


FIG. 2. Plot of initial values $A(K,0)$ (solid curve) and $B(K,0)$ (dashed curve) as a function of K .

corresponding to the decomposition in Eq. (54):

$$\begin{aligned} A(K,t) &= \frac{1}{2}[A^+(K,t) + A^-(K,t)], \\ B(K,t) &= \frac{1}{2}[A^+(K,t) - A^-(K,t)]. \end{aligned} \quad (102)$$

The time evolution of $A^+(K,t)$ is governed by the matrix $\underline{M}^+(K)$, and that of $A^-(K,t)$ by the matrix $\underline{M}^-(K)$. We have chosen the signs such that $A^-(K,0)$ is positive. By expansion in terms of the eigenvectors of $\underline{M}^\pm(K)$, we get

$$A^\pm(K,t) = \sum_{j=1}^{\infty} a_j^\pm(K) \exp[-s_j^\pm(K) D_R t], \quad (103)$$

where $\{s_j^\pm(K)\}$ are the eigenvalues of $\underline{M}^\pm(K)$. It is easy to see that for $K=0$ the matrices $\underline{M}^\pm(0)$ both have the set of eigenvalues $\{s_j^\pm(0)\}$ with $s_j^\pm(0) = 2j^2$. As we shall see, for moderate values of K the low eigenvalues are not much different from the unperturbed eigenvalues $\{s_j^\pm(0)\}$.

In order to find the coefficients $\{a_j^\pm(K)\}$ in Eq. (103), we consider the formal solution of Eq. (77). In vector notation the equation reads

$$s \hat{\mathbf{A}} + \underline{M} \cdot \hat{\mathbf{A}} = \mathbf{h}. \quad (104)$$

The formal solution is

$$\hat{\mathbf{A}}(s) = [s \underline{1} + \underline{M}]^{-1} \cdot \mathbf{h}. \quad (105)$$

This has the spectral decomposition

$$\hat{\mathbf{A}}(s) = \sum_{j=1}^{\infty} \frac{\mathbf{T}_j}{s + s_j}. \quad (106)$$

In components,

$$\hat{A}_l(s) = \sum_{j=1}^{\infty} \frac{T_{lj}}{s + s_j}. \quad (107)$$

By inverse Laplace transformation, we see that the time-dependent vector is given by

$$\mathbf{A}(t) = \sum_{j=1}^{\infty} \mathbf{T}_j \exp[-s_j D_R t]. \quad (108)$$

In components,

$$A_l(t) = \sum_{j=1}^{\infty} T_{lj} \exp[-s_j D_R t]. \quad (109)$$

The time dependence may be summarized in the infinite-dimensional matrix \underline{T} with elements T_{lj} , and the set of eigenvalues $\{s_j\}$. From the initial value $\mathbf{A}(0) = \mathbf{h}$, it follows that the vectors \mathbf{T}_j satisfy the sum rule

$$\sum_{j=1}^{\infty} \mathbf{T}_j = \mathbf{h}. \quad (110)$$

We introduce the constant vector \mathbf{W} with components $W_l(K)$, as defined in Eq. (70). The functions $A^\pm(K,t)$ are given by the scalar products

$$A^\pm(K,t) = \pm \mathbf{W} \cdot \mathbf{A}^\pm(t) = \pm \sum_{j=1}^{\infty} \mathbf{W} \cdot \mathbf{T}_j^\pm \exp[-s_j^\pm D_R t]. \quad (111)$$

The coefficient $a_j^\pm(K)$ in Eq. (103) therefore equals $\pm \mathbf{W} \cdot \mathbf{T}_j^\pm$. In Sec. IX we show how the spectral decomposition may be put to practical use.

IX. ELIMINATION OF FAST VARIABLES

We have not been able to find the explicit eigenvectors of the matrix $\underline{M}(K)$ for arbitrary values of K . However, we can find accurate values of the functions $A^\pm(K,t)$ for moderate values of K by the method of elimination of fast variables [14,15]. We decompose the matrix $\underline{M}(K)$ into submatrices as

$$\underline{M} = \begin{bmatrix} \underline{P} & \underline{Q} \\ \underline{R} & \underline{S} \end{bmatrix}, \quad (112)$$

where \underline{P} is a finite $p \times p$ matrix comprising the first p indices l . The vectors $\hat{\mathbf{A}}(s)$ with components $\{\hat{A}_l(s)\}$ are decomposed correspondingly as $\hat{\mathbf{A}} = (\hat{\mathbf{x}}, \hat{\mathbf{y}})$, where $\hat{\mathbf{x}}$ comprises the first p indices l . For p we use the minimum value 2. The vector \mathbf{h} on the right-hand side of Eq. (104) is decomposed as $\mathbf{h} = (\mathbf{g}, 0)$. Only the first two components of \mathbf{g} are nonvanishing. We can now rewrite Eq. (104) as

$$\begin{aligned} s \hat{\mathbf{x}} + \underline{P} \cdot \hat{\mathbf{x}} + \underline{Q} \cdot \hat{\mathbf{y}} &= \mathbf{g}, \\ s \hat{\mathbf{y}} + \underline{R} \cdot \hat{\mathbf{x}} + \underline{S} \cdot \hat{\mathbf{y}} &= 0. \end{aligned} \quad (113)$$

We eliminate the fast variables $\hat{\mathbf{y}}$ by neglecting the first term in the second equation. This leads to the reduced description

$$s \hat{\mathbf{x}}^{(p)} + \underline{M}_{\text{red}}^{(p)} \cdot \hat{\mathbf{x}}^{(p)} = \mathbf{g}, \quad (114)$$

with the reduced $p \times p$ matrix

$$\underline{M}_{\text{red}}^{(p)} = \underline{P} - \underline{Q} \underline{S}^{-1} \underline{R}. \quad (115)$$

It is clear that the reduced description becomes exact in the limit $p \rightarrow \infty$. The initial value of the vector $\mathbf{x}^{(p)}(t)$,

corresponding to $\hat{\mathbf{x}}^{(p)}(s)$ by inverse Laplace transformation, agrees with the exact value \mathbf{g} for $p \geq 2$. Furthermore, the value of $\hat{\mathbf{x}}^{(p)}(s)$ at $s=0$ agrees with the exact value $\hat{\mathbf{x}}(0)$. In formula,

$$\mathbf{x}^{(p)}(0) = \mathbf{x}(0), \quad \hat{\mathbf{x}}^{(p)}(0) = \hat{\mathbf{x}}(0). \quad (116)$$

The second equality implies that the time integral of $\mathbf{x}^{(p)}(t)$ coincides with the exact value. In practice it suffices to use modest values of p , provided the interaction parameter K is not too large. This method is particularly effective, because the vector \mathbf{h} happens to have a small number of nonvanishing components.

The formal solution of Eq. (114) is given by

$$\hat{\mathbf{x}}^{(p)}(s) = [s\mathbf{I}^{(p)} + \mathbf{M}_{\text{red}}^{(p)}]^{-1} \cdot \mathbf{g}^{(p)}. \quad (117)$$

This can be decomposed as

$$\hat{\mathbf{x}}^{(p)}(s) = \sum_{j=1}^p \frac{\mathbf{T}_j^{(p)}}{s + s_j^{(p)}}. \quad (118)$$

The inverse Laplace transform reads

$$\mathbf{x}^{(p)}(t) = \sum_{j=1}^p \mathbf{T}_j^{(p)} \exp[-s_j^{(p)} D_R t]. \quad (119)$$

The corresponding approximation to the fast variables is given by

$$\mathbf{y}^{(p)}(t) = -\mathbf{S}^{-1} \mathbf{R} \cdot \mathbf{x}^{(p)}(t). \quad (120)$$

These are slaved to the slow variables. The vector $\mathbf{A}(t)$ is approximated by

$$\mathbf{A}^{(p)}(t) = [\mathbf{x}^{(p)}(t), \mathbf{y}^{(p)}(t)].$$

The order p approximation to the functions $A^{\pm}(K, t)$ is given by the scalar product

$$A^{\pm(p)}(K, t) = \pm \mathbf{W} \cdot \mathbf{A}^{\pm(p)}(t). \quad (121)$$

In our case the vector $\mathbf{R} \cdot \mathbf{x}^{(p)}(0)$ vanishes for $p \geq 3$. For such values,

$$A^{\pm(p)}(K, 0) = A^{\pm}(K, 0).$$

In practical calculations we do not need to go beyond $p=4$. The eigenvalues $\{-s_j^{(p)}\}$ are found analytically as roots of the characteristic equation

$$D^{(p)}(s) \equiv |s\mathbf{I}^{(p)} + \mathbf{M}_{\text{red}}^{(p)}| = 0. \quad (122)$$

The determinant is a polynomial of degree p . The matrix elements $T_{ij}^{(p)}$ are found as residues at $-s_j^{(p)}$ from the solution (117) in explicit form by Cramer's rule.

X. CALCULATION OF THE MEMORY FUNCTION

In this section we study the functions $A(K, t)$ and $B(K, t)$ which are related to the memory function by Eq. (72). We consider a limited range of values $0 < |K| < 1.3$, corresponding to an interaction strength $|J|$ of the order of $k_B T$. For larger values the orientations are strongly correlated, which gives rise to sharply peaked orientational distribution functions, requiring a large number of spherical harmonics in their representation. In the range

of values considered, the dynamics of the system may be described in terms of a relatively small number of variables.

We calculate the functions $A(K, t)$ and $B(K, t)$ from the scheme presented in Secs. VIII and IX. As mentioned before, it suffices to consider positive K . In the range $0 < K < 1.3$, the approximation of order $p=4$ in the elimination scheme of Sec. IX does not differ appreciably from the approximation of order $p=3$. Although the higher-order approximation adds the pair of eigenvalues $s_{\pm 4}^{\pm(4)}$, the functions $A^{\pm(4)}(K, t)$ are numerically almost identical to the functions $A^{\pm(3)}(K, t)$. Hence it suffices to consider the approximation of order $p=3$. At $K=1.378$, the eigenvalues $s_{3,4}^{\pm(4)}(K)$ turn complex, indicating a breakdown of the approximation scheme at this point.

In the approximation of order 3, the matrix $\mathbf{M}_{\text{red}}^{\pm(3)}$ reads explicitly

$$\mathbf{M}_{\text{red}}^{\pm(3)} = \begin{pmatrix} 2 \pm K & \mp 2 + 2K & -4 \\ -K & 8 \pm K & \mp 4 + 4K + X^{\pm} \\ 0 & -3K & 18 \pm K + Y^{\pm} \end{pmatrix}, \quad (123)$$

where the additional terms X^{\pm} and Y^{\pm} may be calculated from the matrix $\mathbf{Q}\mathbf{S}^{-1}\mathbf{R}$, as indicated in Eq. (115). The terms are given by

$$\begin{aligned} X^{\pm} &= 60K (\mathbf{S}^{\pm-1})_{44}, \\ Y^{\pm} &= 30K [(\pm 1 - K)(\mathbf{S}^{\pm-1})_{44} + 4(\mathbf{S}^{\pm-1})_{54}]. \end{aligned} \quad (124)$$

The components of the vector $\hat{\mathbf{x}}^{\pm(3)}(x)$ may be calculated from Eq. (117). The components of the vector $\mathbf{y}^{\pm(3)}$ are given by Eq. (120) as

$$y_l^{\pm(3)} = 5K (\mathbf{S}^{\pm-1})_{l4} x_3^{\pm(3)}, \quad l=4, 5, \dots \quad (125)$$

The inverse of the matrix \mathbf{S}^{\pm} may be calculated numerically by truncation at sufficiently high dimension.

The numerical results for the functions $A^{\pm}(K, t)$ can be described in simple terms. It turns out that in the expression (103) only the coefficients $a_1^{\pm}(K)$ and $a_2^{\pm}(K)$ yield an appreciable contribution. Moreover, the ratios $a_{1,2}^+(K)/A^+(K, 0)$ and $a_{1,2}^-(K)/A^-(K, 0)$ hardly vary with K . The ratio $a_1^+(K)/A^+(K, 0)$ tends to $\frac{2}{3}$ as K tends to zero, and the ratio $a_2^+(K)/A^+(K, 0)$ tends to $\frac{1}{3}$. In Fig. 3 we plot the corresponding eigenvalues $s_1^{\pm}(K)$ and $s_2^{\pm}(K)$ as a function of K . These are also practically constant in the range considered. However, the difference $s_1^+(K) - s_1^-(K)$ is crucial for the calculation of the function $B(K, t)$. The functions $A^{\pm}(K, t)$ are approximated very well by a sum of two terms

$$\begin{aligned} A^{\pm}(K, t) &\approx a_1^{\pm}(K) \exp[-s_1^{\pm}(K) D_R t] \\ &\quad + a_2^{\pm}(K) \exp[-s_2^{\pm}(K) D_R t]. \end{aligned} \quad (126)$$

In Fig. 4 we plot the initial values for the corresponding contributions to the functions $A(K, t)$ and $B(K, t)$,

$$\begin{aligned} \alpha_{1,2}(K) &= \frac{a_{1,2}^+(K) + a_{1,2}^-(K)}{2A(K, 0)}, \\ \beta_{1,2}(K) &= \frac{a_{1,2}^+(K) - a_{1,2}^-(K)}{2B(K, 0)}. \end{aligned} \quad (127)$$

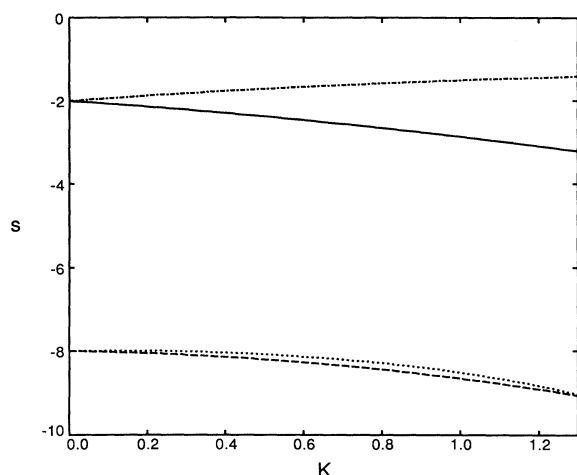


FIG. 3. Plot of the values $-s_1^+(K)$ (solid curve), $-s_2^+(K)$ (dashed curve), $-s_1^-(K)$ (dot-dashed curve), and $-s_2^-(K)$ (dotted curve) as a function of K .

Again, these ratios hardly vary in the range of K considered. All four coefficients are positive. The function $A(K, t)$ decays monotonically to zero, as required by the spectral properties of the two-sphere Smoluchowski operator. On the contrary, the function $B(K, t)$ changes sign as a consequence of the fact that $s_1^-(K) < s_1^+(K)$. The exponential

$$a_1^-(K) \exp[-s_1^-(K) D_R t]$$

dominates at long times. In Fig. 5 we plot the ratios $A(K, t)/A(K, 0)$ and $B(K, t)/B(K, 0)$ as a function of t for $K=1$. The negative tail of the function $B(K, t)$ is conspicuous.

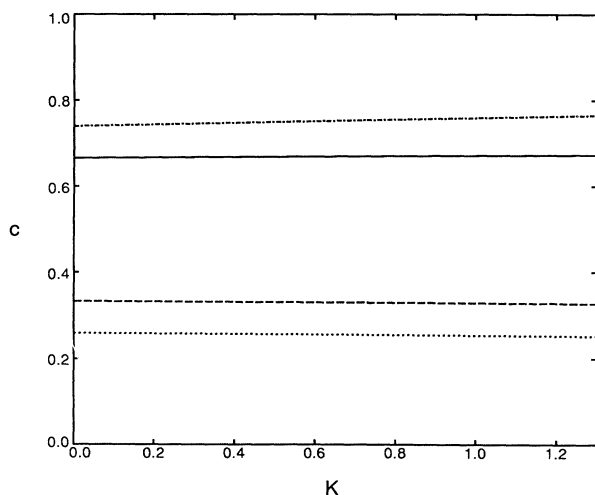


FIG. 4. Plot of contributions to the initial values $A(K, 0)$ and $B(K, 0)$ from coefficients corresponding to different eigenvalues. We plot $\alpha_1(K)$ (solid curve), $\alpha_2(K)$ (dashed curve), $\beta_1(K)$ (dot-dashed curve), and $\beta_2(K)$ (dotted curve), as defined in Eq. (127).

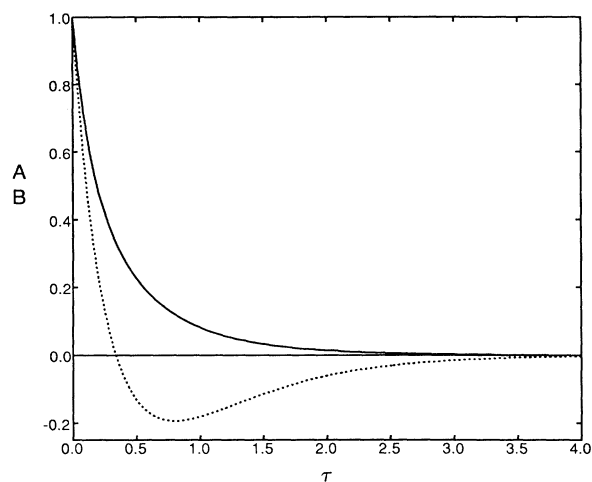


FIG. 5. Plot of the reduced memory functions $A(K, t)/A(K, 0)$ (solid curve) and $B(K, t)/B(K, 0)$ (dotted curve) as functions of $\tau = D_R t$ for $K=1$.

XI. SCATTERING FUNCTION

Upon substitution of the functions $A(K, t)$ and $B(K, t)$ into Eq. (99), one can evaluate the memory function $\mathbf{M}_R(k, t)$. The k dependence of the memory function is determined by the distance dependence of the interactions. In the following we consider the simple model, already studied at the end of Sec. III, for which the interaction $v_0(r)$ vanishes for $r > 2a$ and is infinite for $r < 2a$, and the interaction $J(r)$ takes the constant value J in the range $2a < r < 2x_1 a$ and vanishes elsewhere. For this model we evaluate explicit results for the scattering function.

For the simple model the static structure factors are given by

$$S_I(k) = S_T(k) = 1 + 3\phi Y_1(K) \frac{1}{k^3 a^3} [G(2kax_1) - G(2ka)], \quad (128)$$

with the function

$$G(z) = \sin z - z \cos z. \quad (129)$$

In Fig. 6 we plot $S_I(k)$ as a function of ka for interaction strength $K=1$, range $x_1=2$, and volume fraction $\phi=0.03$. At $k=0$ the factor $S_I(0)$ is less than unity for positive K , and larger than unity for negative K . According to Eq. (29), this implies a speeding up of collective relaxation, as compared with single-particle relaxation, for antiferromagnetic interactions, and a slowing down for ferromagnetic interactions.

To the order of density calculated, the scattering function is isotropic. Its one-sided Fourier transform $\mathbf{G}_R(\mathbf{k}, \omega)$ reduces to a scalar $G_R(k, \omega)$ multiplying the unit tensor. To lowest order in density, the scalar is given by

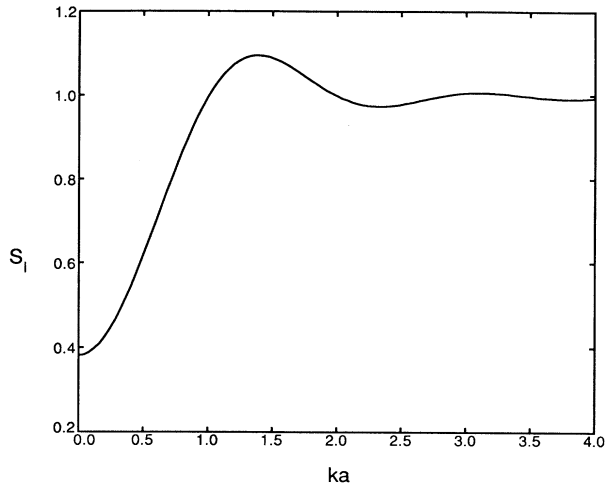


FIG. 6. Plot of the static structure factor $S_l(k)$ as function of ka for $K=1$, $x_1=2$, at volume fraction $\phi=0.03$.

$$G_R(k, \omega) = \frac{1}{3} n_0 \mu^2 \frac{S_l(k)}{-i\omega + 2D_R \{1 + [\lambda_R(k) + \alpha_R(k, \omega)]\phi\}} \quad (130)$$

We have shown above that for moderate values of K the function $\alpha_R(k, \omega)$ may be approximated by a function with four poles on the negative imaginary ω axis, of which the two largest relaxation rates almost coincide. In this approximation the function $G_R(k, \omega)$ has five poles on the negative real s axis, where $s = -i\omega/D_R$, corresponding to roots of the denominator in Eq. (130). In the limit $k \rightarrow 0$, the function $\alpha_R(k, \omega)$ is determined only by $A^+(K, t)$ and may be approximated by a function with only two poles. Correspondingly, in this limit the scalar $G_R(k, \omega)$ may be characterized by only three poles.

Decomposing the function $G_R(k, \omega)$ into partial fractions, we find in the above approximation:

$$G_R(k, \omega) = \frac{1}{3} n_0 \mu^2 S_l(k) \frac{1}{D_R} \sum_{j=1}^5 \frac{c_j(k)}{s - r_j(k)}, \quad (131)$$

with roots $\{r_j(k)\}$ and residues $\{c_j(k)\}$ which satisfy the sum rule

$$\sum_{j=1}^5 c_j(k) = 1. \quad (132)$$

The coefficient $c_4(k)$ corresponds to the root $r_4(k)$, which lies between the two closely spaced poles $-s_2^+(k)$ and $-s_2^-(k)$, and turns out to be negligible.

In our numerical calculations we have replaced the terms $1 + \lambda_R(k)\phi$ in the denominator in Eq. (130) by the complete short-time value $1/S_l(k)$. In Fig. 7 we plot the roots $r_1(k), \dots, r_5(k)$ as a function of ka in the range $0 < ka < 3$ for antiferromagnetic interactions with $K=1$, $x_1=2$, and at volume fraction $\phi=0.03$. In Fig. 8 we plot the coefficients c_1, c_2, c_3 , and c_5 for the same choice of parameters. Both the roots $\{r_j(k)\}$ and the coefficients

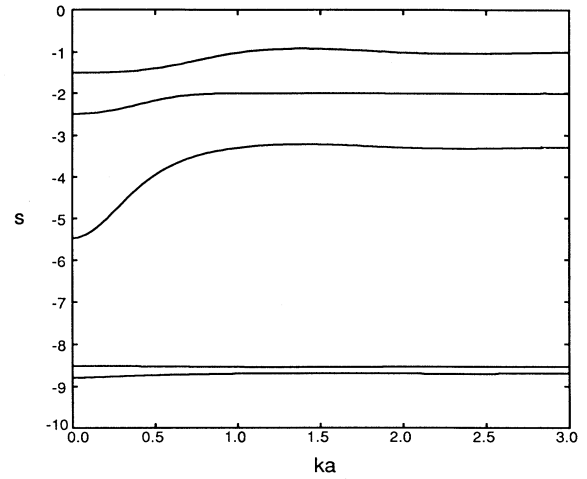


FIG. 7. Plot of poles of the scattering function as a function of ka . We plot $r_1(k), \dots, r_5(k)$ for the Heisenberg model with $K=1$, $x_1=2$, at volume fraction $\phi=0.03$.

$\{c_j(k)\}$ show a strong dependence on wave number. For our choice of parameters, $\lambda_R(0)=20.601$, corresponding to $S_l(0)=0.382$. For comparison,

$$\alpha_R(0,0) = -4(x_1^3 - 1)[\hat{A}(1,0) + \hat{B}(1,0)]$$

takes the value -6.776 . The speeding up of relaxation of long-wavelength modes for strongly antiferromagnetic interactions is manifested by a shift of the weights towards the shorter relaxation times.

Finally, in Fig. 9 we plot the roots r_1, \dots, r_5 as a function of ka for ferromagnetic interactions with $K=-1$, $x_1=2$, at volume fraction 0.03, corresponding to $S_l(0)=1.618$, $\lambda_R(0)=-20.601$, and $\alpha_R(0,0)=-7.879$. In Fig. 10 we plot the corresponding coefficients c_1, c_2 ,

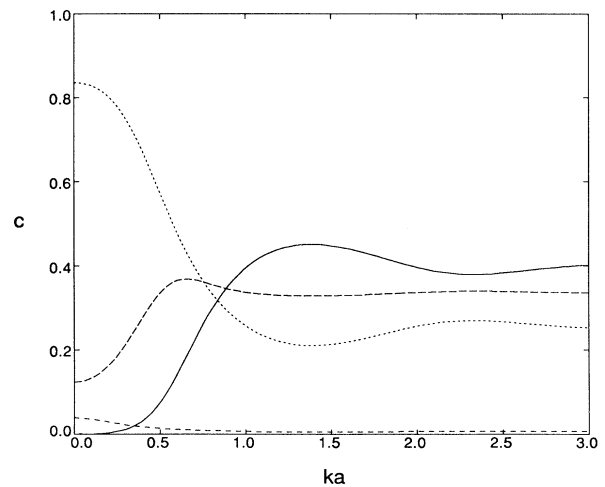


FIG. 8. Plot of the coefficients $c_1(k)$ (solid curve), $c_2(k)$ (long-dashed curve), $c_3(k)$ (dotted curve), and $c_5(k)$ (short-dashed curve), corresponding to the poles plotted in Fig. 7.

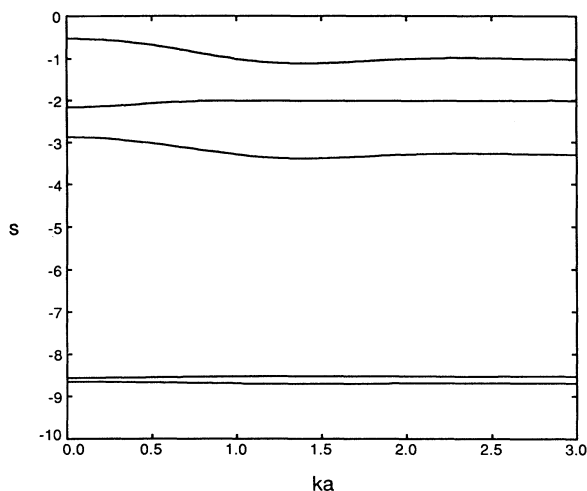


FIG. 9. Same as in Fig. 7 but for $K = -1$.

and c_3 . Again, the coefficients show a strong dependence on wave number. In this case, at small k , the slowest mode gets the largest weight. For small k , the relaxation is dominated by just two modes. The results presented in Figs. 7–10 show a dramatic difference in the collective relaxation between ferromagnetic and antiferromagnetic interactions. The increase of $S_l(k)$ at small k for ferromagnetic interactions indicates a minimum in the free energy for collectively ordered states and signals the approach of the ferromagnetic phase transition. There is a corresponding slowing down in the relaxation of long-wavelength polarization fluctuations. On the contrary, in the case of antiferromagnetic interactions, such long-range correlations are rapidly destroyed.

For the present system, where translational diffusion is neglected, the single-particle orientational correlation function is related to the scattering function at large wave

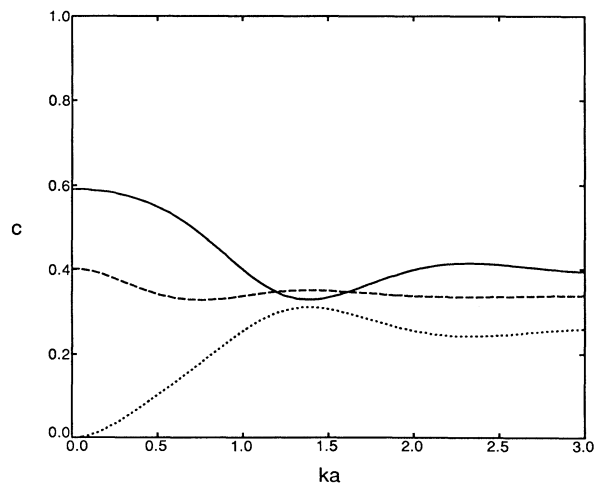


FIG. 10. Plot of the coefficients $c_1(k)$ (solid curve), $c_2(k)$ (dashed curve), and $c_3(k)$ (dotted curve), corresponding to the poles plotted in Fig. 9.

number by

$$C^{(1)}(t) = \frac{3}{\mu^2} \lim_{k \rightarrow \infty} F_R(k, t), \quad (133)$$

as we have shown in Sec. VII. Hence, it follows that for ferromagnetic interactions, the correlation function is well described by a sum of three exponentials, whereas in the case of antiferromagnetic interactions, one needs a sum of four exponentials for an accurate description.

XII. DISCUSSION

We have studied orientational relaxation in the colloidal Heisenberg model with neglect of translational diffusion. We have derived explicit results for the wave-number- and frequency-dependent rotational diffusion coefficient and the single-particle frequency-dependent relaxation time, valid to first order in volume fraction. To this order the memory function characterizing the frequency dependence may be expressed as a radial integral of two contributions, a self-term $A(K, t)$, and a mutual term $B(K, t)$, with $K = J(r)/k_B T$ for distance-dependent Heisenberg interaction $J(r)$. The initial values of these functions can be calculated and are given by Eq. (100). Typically, the initial value of the mutual term is much smaller than the initial value of the self-term. The self-term decays monotonically in time, whereas the mutual term shows an interesting reversal of sign. For Heisenberg interaction of the order $k_B T$, the decay of both functions is well approximated by a sum of four exponentials.

We have studied the rotational dynamic scattering function for a specific model in which the Heisenberg interaction is constant in the range between one and two diameters and vanishes elsewhere. For this model the Fourier transform of the scattering function has a discrete spectrum of poles. For ferromagnetic interactions with $|J|$ of the order of $k_B T$ or less, the scattering function is well approximated by a sum of three exponentials, whereas for antiferromagnetic interactions a sum of four exponentials is needed for accurate description.

For distance-dependent Heisenberg interaction the time dependence of the scattering function is more complicated. Its Fourier transform is characterized by a spectrum in which the discrete poles of the simple model have broadened into continua. It will be of interest to study the time dependence in more detail for various interactions.

Our investigation has revealed that the colloidal Heisenberg model exhibits a rich variety of behavior, even at low volume fraction. The explicit solution we have obtained can serve as a guideline for the study of other systems—for example, polar liquids or ferrocolloids. The Heisenberg model itself deserves further study. We have considered only interactions of limited strength, and it would be desirable to explore the consequences of stronger interactions. Also, it would be of interest to study the effect of translational diffusion.

ACKNOWLEDGMENT

We thank the Deutsche Forschungsgemeinschaft for financial support.

- [1] P. A. Madden, in *Liquids, Freezing and Glass Transition*, edited by J. P. Hansen, D. Levesque, and J. Zinn-Justin (North-Holland, Amsterdam, 1991), p. 547.
- [2] J. P. Hansen and I. R. McDonald, *Theory of Simple Liquids* (Academic, London, 1986).
- [3] C. J. F. Böttcher and P. Bordewijk, *Theory of Electric Polarization* (Elsevier, Amsterdam, 1978), Vol. II.
- [4] S. A. Adelman and J. M. Deutch, *Adv. Chem. Phys.* **31**, 103 (1975).
- [5] J. McConnell, *Rotational Motion and Dielectric Theory* (Academic, London, 1980).
- [6] B. J. Alder and E. L. Pollock, *Annu. Rev. Phys. Chem.* **32**, 311 (1981).
- [7] P. Madden and D. Kivelson, *Adv. Chem. Phys.* **56**, 467 (1984).
- [8] B. Bagchi and A. Chandra, *Adv. Chem. Phys.* **80**, 1 (1991).
- [9] P. N. Pusey and R. J. A. Tough, in *Dynamic Light Scattering and Velocimetry: Applications of Photon Correlation Spectroscopy*, edited by R. Pecora (Plenum, New York, 1982).
- [10] J. A. Montgomery and B. J. Berne, *J. Chem. Phys.* **67**, 4589 (1977).
- [11] R. B. Jones, *Physica A* **150**, 339 (1988).
- [12] B. U. Felderhof and R. B. Jones, *Phys. Rev. E* **48**, 1084 (1993).
- [13] K. H. Fischer and J. A. Hertz, *Spin Glasses* (Cambridge University Press, Cambridge, England, 1991).
- [14] U. Geigenmüller, U. M. Titulaer, and B. U. Felderhof, *Physica A* **119**, 41 (1983).
- [15] N. G. van Kampen, *Phys. Rep.* **124**, 69 (1985).